JOURNAL OF Materials CHEMISTRY

Synthesis and characterisation of mesoporous aluminophosphates containing boron†

Yaroslav Z. Khimyak and Jacek Klinowski*

Department of Chemistry, University of Cambridge, Lensfield Road, Cambridge, UK CB2 1EW. E-mail: jk18@cam.ac.uk; Fax: 01223–33 63 62; Tel: 01223–33 65 14

Received 30th July 2001, Accepted 2nd January 2002
First published as an Advance Article on the web 28th February 2002

Mesostructured and mesoporous boroaluminophosphates (BAPO's) were synthesised using cationic templating in the presence of boric acid. The products were characterised by X-ray diffraction, ^{27}Al, ^{31}P and ^{11}B solid-state NMR, thermal and elemental analysis, and nitrogen adsorption. Boron is incorporated into the structure, leading to a decrease in the degree of condensation of the inorganic component and to reduced thermal stability. Both tetrahedral and trigonal B is present in the structure of as-synthesised and calcined BAPO, but the B(4)–B(3) ratio is significantly reduced upon calcination. The kinetics of product formation were studied, and the likely mechanism of the synthesis is suggested, involving the formation of boroaluminophosphate oligomers which then react with the surfactant cations.

Introduction

Mesoporous and mesostructured solids represent a new class of compounds formed by non-covalent interactions of the surfactant templates with the inorganic component.[1,2] Their structure resembles that of the surfactant mesophases, with the inorganic component arranged around hexagonal, cubic or lamellar surfactant arrays.[3] Since the discovery of mesoporous silicates synthesised in the presence of cationic surfactants (S^+I^- pathway),[4–6] many novel materials have been prepared in the presence of surfactants by cationic (S^+I^- and $S^+M^-I^+$),[3] anionic (S^-I^+)[7,8] or neutral ((S^0I^0)[9–11] and ($S^0H^+M^-I^+$))[12,13] pathways. The products include both silica-based and non-siliceous open framework structures. When the template is removed, some of them yield uniform porous structures, with pore diameters from 20 to 200 Å.

Mesolamellar aluminophosphates (AlPO) were obtained using neutral[14,15] and anionic[16] templating. Non-lamellar mesostructured alumino- and gallophosphates were made using the $AlO_4Al_{12}(OH)_{24}(H_2O)_{12}^{7+}$ and $GaO_4Al_{12}(OH)_{24}(H_2O)_{12}^{7+}$ Keggin ions.[17] Thermally unstable hexagonal mesocomposites were synthesised by ion exchange of Na^+ by $C_{16}H_{33}N(CH_3)_3^+$ in aluminophosphate analogues of the layered mineral kanemite,[18] and by using fluoride anions and organic co-solvents in synthesis mixtures containing cationic surfactants.[19] Kuroda *et al.* reported the synthesis of mesoporous AlPO from aluminium isopropoxide with Al_2O_3 : P_2O_5 = 1.00.[20] In the presence of tetraalkylammonium hydroxides, the supramolecular assembly in the AlPO–C_{16}TMACl system gives mesocomposites with different structures and properties.[21–23] X-Ray diffraction (XRD) allowed us to identify three hexagonal (Hex-1, Hex-2, Hex-3) and three mesolamellar (L1, L2 and L3) products. The inorganic component of mesostructured AlPO's varies in the degree of condensation, the P : Al ratio and the population ratio of 6- and 4-coordinate Al. The $C_{16}TMA^+$ cations are the only organic species in the products. The differences in the mesocomposites are also reflected in the specific organisation of the surfactant arrays. Thus, at ambient temperatures, Hex-1, Hex-2 and L2 show a predominant disordered *gauche* conformation of the aliphatic chains, while in L1 and L3 they are in the all-*trans* conformation.[24] Upon template removal, Hex-1 and Hex-2 give mesoporous solids with tubular pore arrangements.[23]

Incorporation of boron into open-framework solids has been reported for zeolites, microporous AlPO and mesoporous MCM-41 silicates.[25–28] Depending on the synthesis conditions and framework type, boron was shown by ^{11}B MAS NMR to be in either tetrahedral or trigonal environments. The framework BO_4–BO_3 ratio depends on the degree of hydration of the sample. Incorporation of boron into the framework of porous solids is expected to have an effect on their acidic properties and hence on their catalytic activity.

Following previous studies on the synthesis and structure of mesostructured and mesoporous AlPO, silicoaluminophosphate (SAPO), magnesiophosphate (MgAPO) and MgAPSO,[23,29] we describe the synthesis and characterisation of B-modified mesostructured and mesoporous AlPO's. Kevan and co-workers obtained and characterised mesoporous AlPO containing manganese and vanadium.[30,31] Mesoporous SAPO has also been obtained.[32,33] However, no systematic studies have been performed on the incorporation mechanism of the different heteroatoms in the structure, and on the comparison between heteroatom-substituted microporous and mesoporous aluminophosphates. We have studied the direct incorporation of boron atoms into mesostructured AlPO using an array of techniques. In comparison with other heteroatoms, boron offers an opportunity to study the process of isomorphous substitution, since the status of B can be monitored directly at different stages of the synthesis by ^{11}B solid-state NMR. The results of studies of the synthesis intermediates are also described.

Experimental

Synthesis

Synthesis of hexagonal BAPO was carried out at ambient conditions. In the first step, $Al(OC_3H_7^{iso})_3$ was dispersed in water and stirred for 30 min. The required amount of H_3PO_4 was then added (P_2O_5 : Al_2O_3 = 2.0) and the mixture was stirred for 60 min. A boron source (H_3BO_3, Aldrich) was added

†Electronic supplementary information (ESI) available: thermogravimetric analysis of mesostructured BAPO,XRD patterns of Hex-2 BAPO,^{27}Al MAS NMR spectra of intermediate products formed during the synthesis of Hex-1 BAPO, ^{11}B MAS NMR spectra of Hex-2 BAPO. See http://www.rsc.org/suppdata/jm/b1/b106911j/

to the synthesis mixture. A solution of cetyltrimethylammonium‡ chloride (CTAC) (Aldrich) was then added. After stirring for 1 h, a 25% aqueous solution of tetramethylammonium hydroxide (TMAOH) (Lancaster) was added dropwise. The mixtures were magnetically stirred during the whole course of the synthesis. After 48–96 h the products were filtered and dried at 50 °C overnight. The products were calcined at 500 °C in air for 12 h. They are referred to as BAPO[B-*n*], where *n* is the Al : B ratio in the synthesis mixture. The composition of the starting mixtures used for the synthesis of hexagonal BAPO was as follows: 1.0 Al_2O_3 : 2.0 P_2O_5 : 1/*n* B_2O_3 : 0.71 CTAC : *m* TMAOH : *k* H_2O, *n* = 25.0–2.0, *m* = 4.22 for Hex-1 and 4.61 for Hex-2, *k* = 320 for Hex-1 and 330 for Hex-2.

Powder X-ray diffraction

XRD patterns were recorded using a Philips 1710 powder diffractometer with Cu-Kα radiation (40 kV, 40 mA), 0.020° step size and 0.5–2.0 s counting time per step.

Solid-state NMR

NMR spectra were recorded at 9.4 T using a Chemagnetics CMX-400 spectrometer. ^{27}Al magic-angle-spinning (MAS) NMR spectra were acquired at 104.20 MHz with pulses shorter than π/10 (0.3 μs pulse length) using zirconia rotors 4 mm in diameter spun in dry nitrogen at 8 kHz. 1000 scans were acquired with a recycle time of 0.5 s. The position of ^{27}Al resonances is quoted in ppm from external $Al(H_2O)_6^{3+}$. ^{31}P MAS NMR spectra were measured at 161.89 MHz with zirconia rotors 7.5 mm in diameter spun in nitrogen at 5.5 kHz, π/2 (6.5 μs) pulses, 8 scans and 120 s recycle delays. ^{31}P chemical shifts are quoted with respect to external 85% H_3PO_4. ^{11}B MAS NMR spectra were measured at 128.30 MHz with π/6 pulses (0.30 μs pulse length) using zirconia rotors 4 mm in diameter spun at 11.0 kHz. 2000 scans were acquired with a recycle time of 1.0 s. ^{1}H – ^{11}B CP/MAS NMR spectra were acquired using ^{1}H π/2 (4.2 μs) pulses at 399.88 MHz. The Hartmann–Hahn condition was established using boric sodium borate and verified using as-synthesised Hex-1 BAPO with the highest content of B. The spectra were acquired at different contact times (t_m = 0.02–16.0 ms) using a 5.0 s recycle delay. The number of transients varied in the 1600–2400 range, depending on the signal-to-noise ratio.

Thermogravimetry

Thermogravimetric (TG) analysis was carried out using a Polymer Laboratories TGA 1500 instrument under a flow of nitrogen, with a heating rate of 10 °C min^{-1} in the 20–800 °C temperature range.

Elemental analysis

Samples were analysed for carbon, hydrogen and nitrogen using a Carlo Erba elemental analyser. Phosphorus was determined colorimetrically. JEOL 5800 and JEOL 2101 scanning electron microscopes with energy-dispersive X-ray (EDS) attachments, operating at 15 kV and 200 kV respectively, were used to determine the Al : P ratio.

N_2 adsorption–desorption

Nitrogen adsorption–desorption measurements were carried out using the volumetric method with a Coulter SA3100 sorptometer at −196 °C. Before analysis, calcined samples were dried at 120 °C and evacuated for 8 h at 200 °C. The surface area was calculated using the BET method on the basis of the adsorption branch in the 0.05–0.20 partial pressure (p/p_0) range. Pore volume was determined from the amount of N_2 adsorbed at p/p_0 = 0.99. Pore size was calculated using the Horvath–Kawazoe method.[34]

Results and discussion

Synthesis, composition and XRD

The synthesis of boron-modified mesostructured AlPO's was carried out using starting mixtures containing boric acid as a source of boron with Al : B = 2.5–25.0. In contrast to the syntheses of hexagonal MgAPO and SAPO,[23,29] the pH of the synthesis mixture is virtually unchanged by the B content. The pH of the synthesis was 7.26–7.32 for Hex-1 and 7.60–7.70 for Hex-2.

XRD patterns of the mesostructured BAPO's feature (100), (110) and (200) reflections typical of a two-dimensional hexagonal network. Hex-1 BAPO's give relatively narrow diffraction peaks with d_{100} = 39.7–40.5 Å (Fig. 1). The quality of the mesostructure remains unchanged even for the highest amount of B in the synthesis mixture, as indicated by the intensities of both (100) and (110) reflections. Slightly broader (100) peaks are observed for Hex-2 BAPO's (XRD patterns are given in the Electronic Supplementary Information).† The B content of the synthesis mixture does not affect the d_{100} spacing for either Hex-1 or Hex-2 BAPO's. The XRD patterns of calcined Hex-1 and Hex-2 BAPO's indicate a much higher thermal stability for Hex-1 BAPO's (Fig. 2) in comparison with Hex-2 BAPO's. The intensities of the diffraction peaks of Hex-1 BAPO are higher and the peaks are narrower.

Three main thermal events are observed during the calcination of mesostructured aluminophosphates.[23] The first, at 90–110 °C, is related to the loss of water (physisorbed water at 80–90 °C and chemisorbed water at 100–110 °C). The second and third steps, at 250–270 and 330–370 °C, respectively, are attributed to the decomposition of the template. TG analysis indicates that, unlike mesostructured MgAPO or SAPO,[29] whose template content decreases with rising heteroatom content, increasing the B content in the synthesis mixture has practically no influence on the total weight loss. For Hex-1 BAPO obtained with a broad range of B contents, the total weight loss is 59.0–61.0%, while for Hex-2 the same parameter is larger and amounts to 65.0–67.0% (details of TG analysis are given in the ESI).† Hex-2 BAPO's show a higher relative contribution of the second step in the TG curve.

EDS analysis was used to determine the Al : P ratios in the

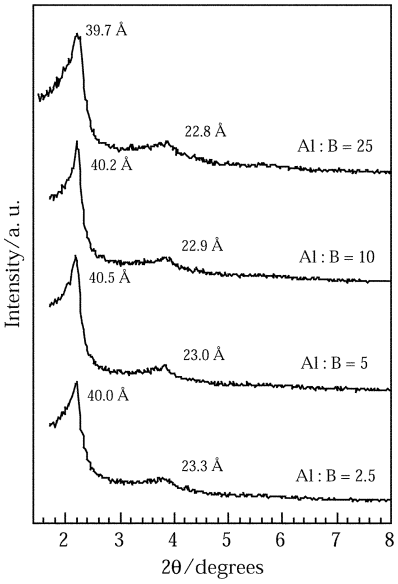

Fig. 1 XRD patterns of Hex-1 BAPO.

‡The IUPAC name for cetyl is hexadecyl.

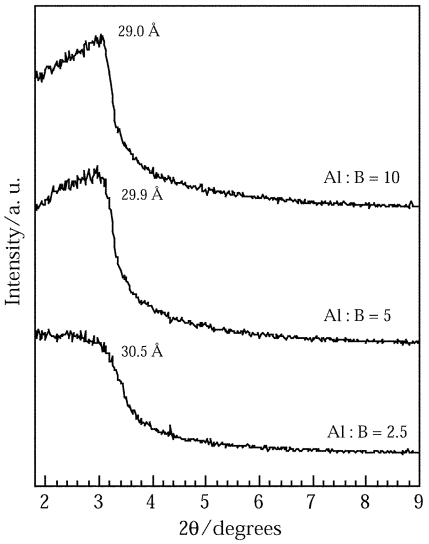

Fig. 2 XRD patterns of Hex-1 BAPO calcined at 500 °C.

solids. For Hex-1 BAPO Al : P decreases slightly with the increase in B content from 0.87 for Hex-1 BAPO[B-10.0] to 0.82 for Hex-1 BAPO[B-2.5]. A similar effect is found in Hex-2 BAPO with different B contents. We also note that the Al : P ratio in mesoporous MgAPO and SAPO changes slightly upon the incorporation of heteroatoms.[29]

Nitrogen adsorption

Higher thermal stability of Hex-1 BAPO in comparison with Hex-2 BAPO is confirmed by nitrogen adsorption (see Table S1)†, as calcined Hex-1 BAPO's show a much higher surface area and pore volume than Hex-2 BAPO's obtained at the same Al : B ratios. Increasing the boron content in the synthesis mixture reduces both S_{BET} and V_{ads} for both Hex-1 and Hex-2 BAPO's. The general appearance of the adsorption–desorption isotherms, and the pore diameter in the solids, does not vary significantly with B content.

Comparison of the N_2 adsorption–desorption parameters of mesoporous BAPO's with those for MeAPO's suggests that mesoscopic ordering of calcined Hex-1 BAPO's is comparable to that of mesoporous AlPO's, MgAPO's and MgAPSO's. Moreover, the values of S_{BET} and V_{ads} for BAPO's obtained at Al : B < 5.0 are larger than those for the MeAPO's obtained at the same Al : Me ratio.[29] Much lower values of S_{BET} and V_{ads} for calcined Hex-2, compared to calcined Hex-1 BAPO with the same Al : B ratio, indicate a much lower quality of tubular pore system in the former.

^{27}Al and ^{31}P MAS NMR

^{27}Al MAS NMR spectra of mesostructured BAPO's indicate a predominantly octahedral coordination for aluminium. Al(6) is found at −(4.9–5.6) ppm for Hex-1 and −(3.0–3.8) ppm for Hex-2 BAPO (Fig. 3). Increasing the B content reduces the Al(4)–Al(6) ratio in both Hex-1 and Hex-2. Thus, for Hex-1 BAPO's, decreasing Al : B in the synthesis mixture from 10.0 to 2.0 reduces the Al(4)–Al(6) ratio from 0.40 to 0.30. In general, the ^{27}Al MAS NMR spectra of mesostructured BAPO are typical of those of hexagonal AlPO.[23] Practically no change of the Al(4)–Al(6) ratio was observed for the Mg and Zn incorporated AlPO.[29,35] On the other hand, the introduction of Si into the framework significantly increases the contribution of Al(4).[29,32]

The ^{31}P MAS NMR spectra of Hex-1 and Hex-2 BAPO resemble those of the corresponding hexagonal AlPO.[23] For Hex-1 BAPO's, the spectra consist of several overlapping

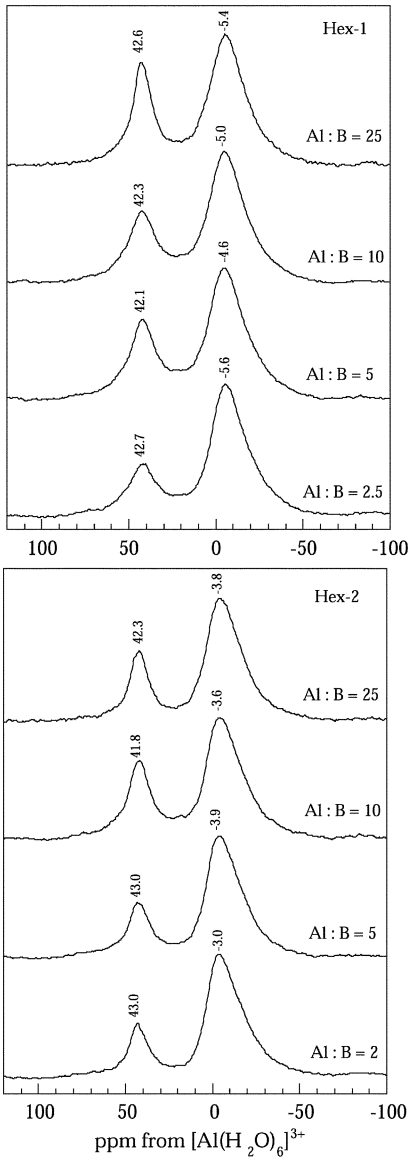

Fig. 3 ^{27}Al MAS NMR spectra of Hex-1 and Hex-2 BAPO's.

resonances with the main broad line at −(11.7–14.1) ppm and a relatively sharp resonance at *ca.* –2.5 ppm (Fig. 4). The position of the sharp peak is shifted upfield by 1.7 ppm in comparison with Hex-1 AlPO. Analysis of the ^{31}P MAS NMR and ^{1}H–^{31}P CP/MAS dynamics in mesostructured AlPO[36] indicates that this resonance can be ascribed to P atoms, with a very low degree of condensation, connected to the surfactant species. The fact that for Hex-1 and Hex-2 BAPO this resonance is shifted upfield, suggests that B is incorporated into the framework and is located very close to the inorganic–organic border. For Hex-1 BAPO's the relative intensity of the peak at −2.5 ppm increases with increasing B content. For Hex-2 the ^{31}P MAS NMR confirms a less condensed inorganic framework, formed around the surfactant arrays, as the most intense peaks are found at −(1.2–2.1) ppm (Fig. 5). The broad resonance at *ca.* −12.0 ppm represents several kinds of ^{31}P sites with different degrees of condensation of the inorganic framework. As has been shown by ^{31}P MAS NMR and ^{1}H–^{31}P CP/MAS dynamics in mesostructured AlPO's, the upfield shift of the ^{31}P resonances corresponds to the increased degree of condensation of the inorganic framework.[23,36]

In contrast to hexagonal MgAPO, SAPO and MgAPSO synthesised at different Al : Mg and Al : Si ratios,[29,32] boron-substituted aluminophosphates show a decreased degree of

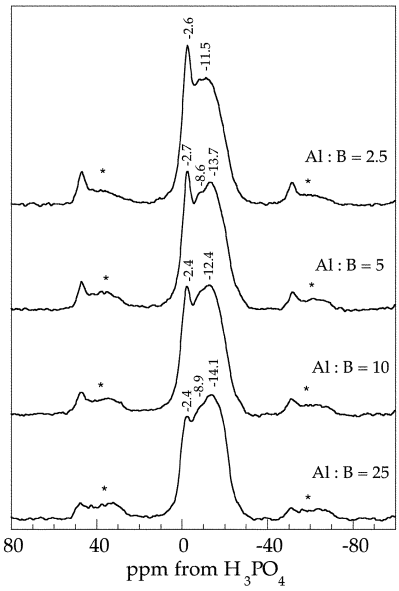

Fig. 4 ^{31}P MAS NMR spectra of Hex-1 BAPO's. Asterisks denote spinning sidebands.

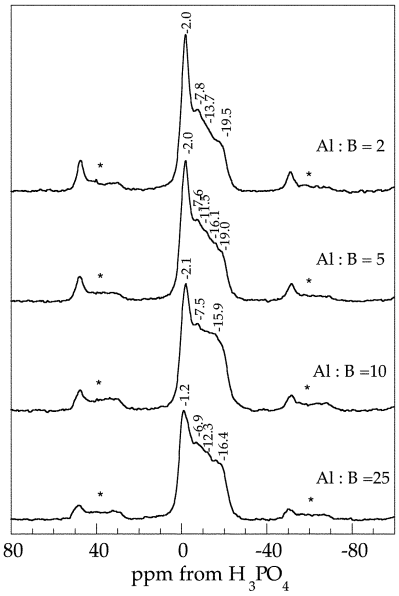

Fig. 5 ^{31}P MAS NMR spectra of Hex-2 BAPO's. Asterisks denote spinning sidebands.

condensation of the inorganic component with increasing boron content. Introduction of boron into the structure has little effect on the Al(4) : Al(6) ratio, an effect also observed for MgAPO where aluminium is substituted by magnesium. It is clear that modification by boron proceeds by a mechanism entirely different from that governing incorporation of silicon, where significant changes in host structure were monitored by both ^{27}Al and ^{31}P MAS NMR and there was a substantial increase in the degree of condensation.

^{11}B MAS NMR

The ^{11}B MAS NMR spectra of hexagonal BAPO's reveal two kinds of B sites in the structure (Fig. 6). The first represents B atoms with tetrahedral coordination (0.1–0.3 ppm) and is characterised by a narrow intense peak. The second broad peak at 13.5 ppm comes from B in the trigonal coordination. The relative contribution of trigonal B is higher in Hex-2 than in Hex-1, and increases with increasing B content. Integrals of the

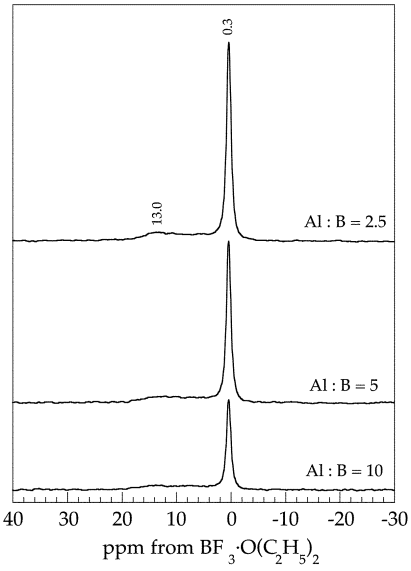

Fig. 6 ^{11}B MAS NMR spectra of Hex-1 BAPO's.

peaks show that, for both Hex-1 and Hex-2, the B incorporated into the AlPO framework is proportional to that in the synthesis mixture.

We note that similar ^{11}B MAS NMR spectra have been reported for mesoporous borosilicate molecular sieves.[25–28] The state of ^{11}B in the molecular sieves is generally described by a relatively narrow range of chemical shifts. For mesoporous and mesostructured [Si, B]MCM-41, tetrahedral ^{11}B is observed from 2.0 to −3.0 ppm. The peaks in the tetrahedral region are likely to represent a superposition of peaks arising from $B(OSi)_{4-x}(OH)_x$ sites.[37] Mesostructured [Si, B]MCM-41 described by Liu *et al.* contains two kinds of ^{11}B sites at −1.0 and −2.5 ppm.[26] The former was assigned to $B(OSi)_3OH$ units, and the latter to $B(OSi)_4$ units. Generally, the chemical shift of ^{11}B in the mesostructured BAPO's alone cannot be used to form a definite conclusion about the second coordination sphere of boron. As in mesostructured borosilicates, the presence of water and template molecules may influence the ^{11}B chemical shift and linewidth.[37]

^{1}H–^{11}B CP/MAS spectra of mesostructured BAPO, registered with relatively short contact times, are dominated by the B(3) peak (Fig. 7) with maximum intensity for $t_m = 0.5$ ms. For B(4), much longer contact times (t_m = 2–4 ms) are required. The faster ^{1}H–^{11}B CP/MAS dynamics for the peak at *ca.* 13.0 ppm may indicate that 3-coordinate boron atoms are closer to protons than 4-coordinate atoms. One can assume that B–OH groups are absent from the B(4) units. However, one should also consider that much slower polarisation transfer to tetrahedral boron may result from close proximity to a very mobile proton source, such as the N–CH_3 groups.[24] We therefore suggest that $BO_4^{-}\cdot{}^{+}N(CH_3)_3C_{16}H_{33}$ units are present in the structure.

The spectra of calcined BAPO's are different and much broader than the spectra of their mesostructured precursors (Fig. 8), and similar to those of the calcined mesoporous borosilicates.[26,37] Analysis of the spectra is hampered by the overlapping peaks. We note that much better resolved ^{11}B solid-state NMR spectra of amorphous solids can be measured using either stronger magnetic field or much faster MAS. Thus B(3) and B(4) sites in glasses can be completely resolved at fields above 11.7 T due to the significant reduction of the quadrupolar interactions.[38] Nevertheless, even at 9.4 T it is clear that, in contrast to as-synthesised solids, most of the boron in the structure is in the trigonal coordination (11.6–11.9 ppm). The solids also contain tetrahedral B at 0.1 ppm. Trigonal B is produced from tetrahedral B by removal of the

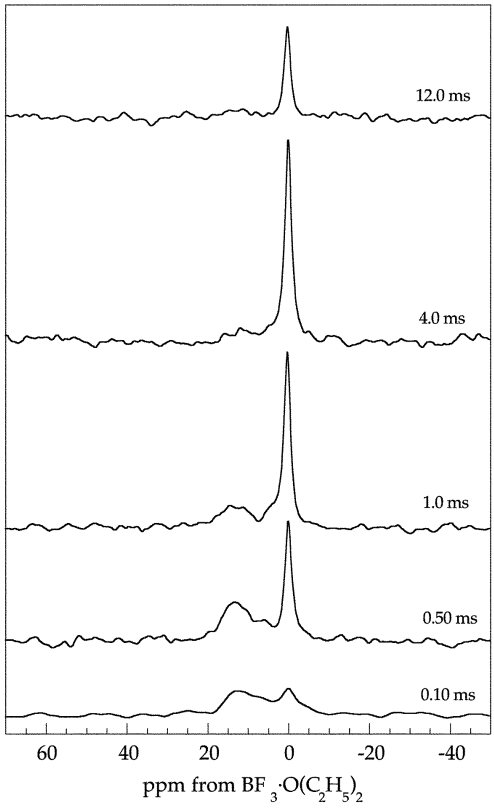

Fig. 7 ^{1}H–^{11}B CP/MAS spectra of Hex-1 BAPO.

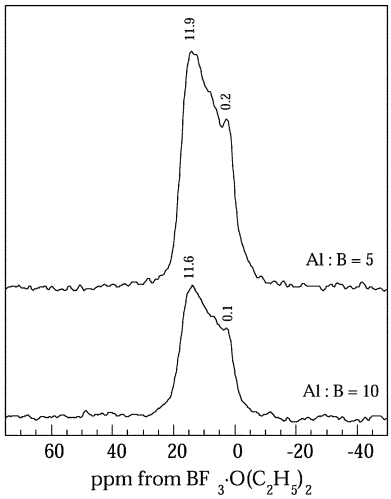

Fig. 8 ^{11}B MAS NMR spectra of calcined Hex-1 BAPO.

surfactant cations from the structure. However, it is clear that even after 12 h calcination at 500 °C in air, B(4) remains in the structure.

As in as-synthesised samples, B(3) shows faster ^{1}H–^{11}B CP/MAS kinetics than B(4) (Fig. 9). The latter become dominant in the spectra recorded with longer contact time. However, the maxima on the variable-contact-time curves for B(4) are observed at much shorter t_m than for the as-synthesised samples. This is clearly related to the different proton source. For calcined samples, this consists of the protons of the hydroxy groups connected to the nearby phosphorus or aluminium atoms. Still, the protons are located further from B(4) units than from B(3) units.

^{11}B MAS NMR spectra of amorphous BAPO with no surfactant incorporated, and obtained using synthesis mixtures containing only $\frac{1}{3}$ of the TMAOH required for the synthesis of

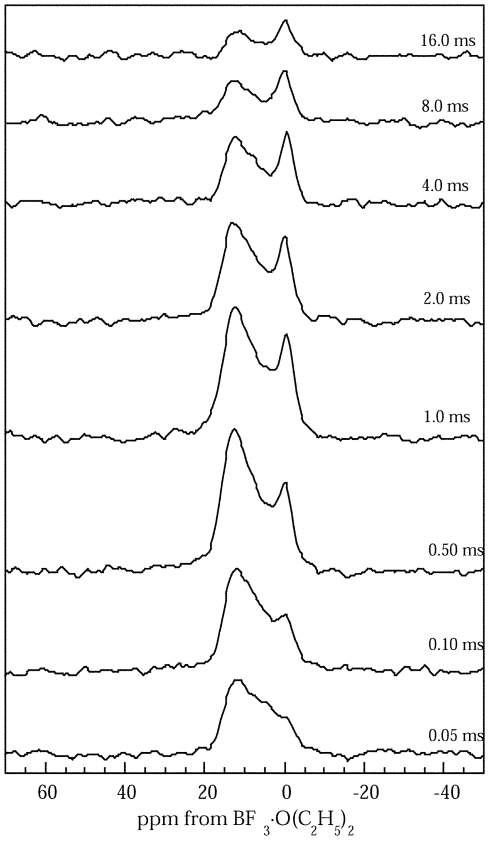

Fig. 9 ^{1}H–^{11}B CP/MAS spectra of calcined Hex-1 BAPO.

Hex-1 BAPO, show only one peak at −1.6 ppm attributable to B(4). Its CP dynamics are significantly faster than those of B(4) in either as-synthesised or calcined Hex BAPO's, but still slower than for B(3). Much faster ^{1}H–^{11}B CP/MAS dynamics for B(4) can be attributed to a lower mobility of the ^{1}H reservoir compared to that in the Hex-1, which is consistent with the absence of the surfactant from the structure.

We note that the results of the CP dynamics of quadrupolar nuclei should be treated with caution, as the process is much more complex than for ½ spin nuclei, because of the presence of multiple nutation rates, several of which may be matched by the ^{1}H nutation rate. The sites with markedly different values of the quadrupolar coupling constant and asymmetry parameter may have significantly different CP characteristics and exhibit matching conditions at different field strengths.[39,40] Based on the CP dynamics, we assume that in the mesostructured and mesoporous BAPO, trigonal B sites are located closer to the source of protons than the tetrahedral sites. This conclusion agrees with the results of the $^{11}B\{^{1}H\}$ rotational echo double resonance experiments (REDOR) for the B-ZSM-5. In this case, the REDOR effect for B(3) is stronger than for B(4), because of the short ^{11}B–^{1}H distance in the B(3)···O(H)-Si groups.[28,41]

Kinetics of formation of mesostructured BAPO's

Regularities of the formation of mesostructured BAPO were examined using the intermediate solids collected at different stages of synthesis. The experiments were performed using synthesis mixtures with high boron content (Al : B = 2.0). XRD shows the presence of mesostructured products only 15 min after the addition of TMAOH. The quality of the solids increases with the duration of the reaction, resembling the pattern observed for the formation kinetics of Hex-1 AlPO.[23]

^{27}Al MAS NMR of the intermediate products shows a decrease in the Al(4)–Al(6) ratio with synthesis time. Compared to the synthesis of Hex-1 AlPO, the contribution of

tetrahedral Al is lower in the structure of solids collected after 15 min synthesis. This may be due to the introduction of B atoms in the AlPO building units formed during early steps of the reaction. A significant decrease of the Al(4)–Al(6) ratio is observed after 1.5–2.0 h of synthesis. The Al(4)–Al(6) ratio decreases from 0.53 after 15 min to 0.20 after 48 h. ^{27}Al MAS NMR spectra are given in the ESI.

The relative contribution of the narrow peaks at *ca.* −2.5 ppm in the ^{31}P MAS NMR spectra gradually increases, while the position of the broad peak shifts downfield from *ca.* −15.3 ppm for the solids obtained after 15 min to *ca.* −11.0 ppm after 20 h (Fig. 10). As expected, the relative contribution of the resonance at the lowest field in Hex-1 BAPO is larger than in Hex-1 AlPO. We note that the position of the resonance at −2.5 ppm does not change with time, indicating that incorporation of B, responsible for the upfield shift compared with Hex-1 AlPO, takes place before formation of the mesostructured solid.

Studies of the formation kinetics of Hex-1 BAPO can also give information on the status of the heteroatoms during different stages of the synthesis. ^{11}B MAS NMR spectra of solids obtained after 15 min of synthesis contain resonances from both trigonal and tetrahedral B. The relative contribution of B(3) decreases during the synthesis (Fig. 11(a)). The relative intensity of the peaks is high for solids collected after only 15 min synthesis, indicating a high degree of B incorporation.

Intense resonances in the ^{11}B MAS NMR spectra of solids, obtained with different TMAOH contents in the synthesis mixture (Fig. 11(b)), indicate that introduction of boron into the aluminophosphate network takes place during early stages of the synthesis and does not require the presence of TMAOH. The spectra of amorphous BAPO synthesised without TMAOH, or with only $\frac{1}{3}$ of the TMAOH required for the formation of Hex-1 BAPO, contain a single peak at −1.6 ppm attributable to B(4). Increasing the quantity of TMAOH causes significant changes in the spectra. Thus, spectra of BAPO synthesised using $\frac{2}{3}$ of the amount of TMAOH are similar to those of Hex-1 BAPO. However, an increased contribution of B(3) is observed. The downfield shift of the peak, corresponding to B(4) units, with increasing TMAOH content, can be related to bond formation between the boron sites and the surfactant. We therefore suggest the following scheme of synthesis. Aluminophosphate complexes formed after mixing $Al(OC_3H_7^{iso})_3$–H_2O slurry with H_3PO_4 are capable of including BO_4 structural units in their structure in the acidic medium, giving boroaluminophosphate oligomers. Upon addition of TMAOH these then react with the surfactant cations. As a result, a reorganisation of the inorganic component takes place, as some of the B atoms are found in trigonal units while others remain in the tetrahedral coordination. The relative contribution of B(3) decreases as the reaction progresses.

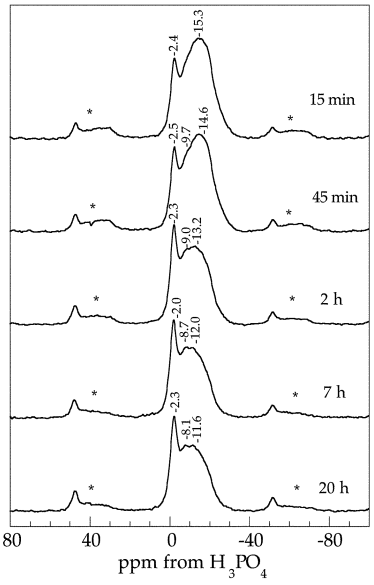

Fig. 10 ^{31}P MAS NMR spectra of intermediate products formed during the synthesis of Hex-1 BAPO. Asterisks denote spinning sidebands.

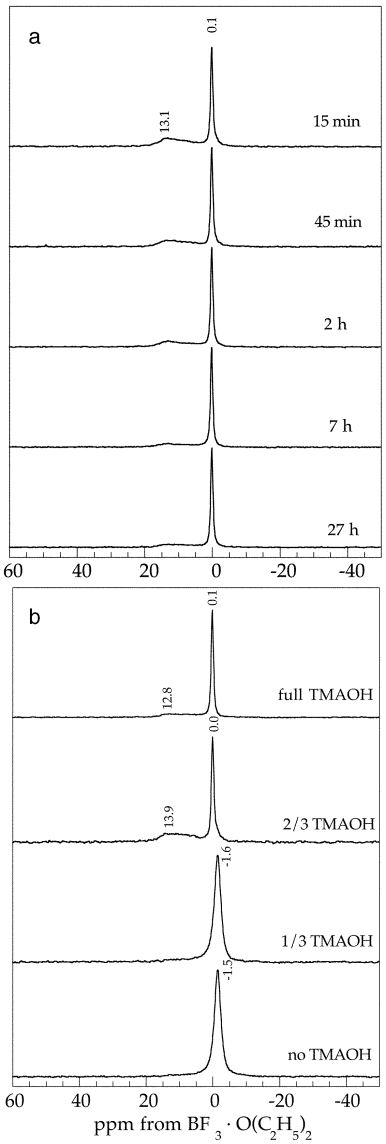

Fig. 11 ^{11}B MAS NMR spectra of Hex-1 BAPO collected at (a) different reaction times and (b) different TMAOH content.

Conclusions

Mesostructured and mesoporous aluminophosphates containing boron were synthesised at ambient temperature using a cationic surfactant. The structure of the mesostructured solids resembles that of Hex-1 and Hex-2 AlPO, with a fairly low degree of condensation of the inorganic component. Incorporation of boron in the structure has been demonstrated by ^{31}P and ^{11}B MAS NMR. Increasing the B content reduces the degree of condensation of the inorganic network indicated by the increased contribution of units connected to the template and by reduced thermal stability. In mesostructured BAPO, boron is mainly in the tetrahedral coordination. Trigonal B is also present. Most probably, the latter is closer to the protons than B(4).

Removal of the surfactant by calcination gives porous solids

with a tubular pore arrangement. The quality of the pore system decreases with increasing B content. However, calcined Hex-1 BAPO with Al : B $\geqslant$ 5.0 have high surface area and pore volume. Both B(3) and B(4) are present in the structure after calcination, although the contribution of the B(3) units is much larger than in the initial mesostructured BAPO.

Studies of the formation kinetics of mesostructured BAPO show that incorporation of B into the inorganic component takes place during the early stages of synthesis and does not require the presence of the organic bases or of the surfactant. As a result, boroaluminophoshate oligomers with boron in the tetrahedral coordination are formed.

Acknowledgement

We are grateful to the Cambridge Oppenheimer Fund for the Research Fellowship for Y. K.

References

1 J. S. Beck, J. C. Vartuli, W. J. Roth, M. E. Leonowicz, C. T. Kresge, K. D. Schmitt, C. T. W. Chu, D. H. Olson, E. W. Sheppard, S. B. McCullen, J. B. Higgins and J. L. Schlenker, *J. Am. Chem. Soc.*, 1992, **114**, 10834.
2 A. Corma, *Chem. Rev.*, 1997, **97**, 2373.
3 Q. S. Huo, D. I. Margolese and G. D. Stucky, *Chem. Mater.*, 1996, **8**, 1147.
4 J. S. Beck, J. C. Vartuli, G. J. Kennedy, C. T. Kresge, W. J. Roth and S. E. Schramm, *Chem. Mater.*, 1994, **6**, 1816.
5 C. F. Cheng, Z. H. Luan and J. Klinowski, *Langmuir*, 1995, **11**, 2815.
6 S. Inagaki, Y. Yamada, Y. Fukushima and K. Kuroda, *Stud. Surf. Sci. Catal.*, 1995, **92**, 143.
7 N. K. Raman, M. T. Anderson and C. J. Brinker, *Chem. Mater.*, 1996, **8**, 1682.
8 F. Vaudry, S. Khodabandeh and M. E. Davis, *Chem. Mater.*, 1996, **8**, 1451.
9 P. T. Tanev and T. J. Pinnavaia, *Science*, 1995, **267**, 865.
10 S. A. Bagshaw, E. Prouzet and T. J. Pinnavaia, *Science*, 1995, **269**, 1242.
11 E. Prouzet and T. J. Pinnavaia, *Angew. Chem., Int. Ed.*, 1997, **36**, 516.
12 D. Zhao, Q. Huo, J. Feng, B. F. Chmelka and G. H. Stucky, *J. Am. Chem. Soc.*, 1998, **120**, 6024.
13 Y. Z. Khimyak and J. Klinowski, *J. Mater. Chem.*, 2000, **10**, 1847.
14 S. Oliver, A. Kuperman, N. Coombs, A. Lough and G. A. Ozin, *Nature*, 1995, **378**, 47.
15 A. Sayari, I. Moudrakovski, J. S. Reddy, C. I. Ratcliffe, J. A. Ripmeester and K. F. Preston, *Chem. Mater.*, 1996, **8**, 2080.
16 M. Froba and M. Tiemann, *Chem. Mater.*, 1998, **10**, 3475.
17 B. T. Holland, P. K. Isbester, C. F. Blanford, E. J. Munson and A. Stein, *J. Am. Chem. Soc.*, 1997, **119**, 6796.
18 S. F. Cheng, J. N. Tzeng and B. Y. Hsu, *Chem. Mater.*, 1997, **9**, 1788.
19 P. Y. Feng, Y. Xia, J. L. Feng, X. H. Bu and G. D. Stucky, *Chem. Commun.*, 1997, 949.
20 T. Kimura, Y. Sugahara and K. Kuroda, *Chem. Mater.*, 1999, **11**, 508.
21 Y. Z. Khimyak and J. Klinowski, *Chem. Mater.*, 1998, **10**, 2258.
22 Y. Z. Khimyak and J. Klinowski, *J. Chem. Soc., Faraday Trans.*, 1998, **94**, 2241.
23 Y. Z. Khimyak and J. Klinowski, *Phys. Chem. Chem. Phys.*, 2000, **2**, 5275.
24 Y. Z. Khimyak and J. Klinowski, *Phys. Chem. Chem. Phys.*, 2001, **3**, 616.
25 F. S. Xiao, S. L. Qiu, W. Q. Pang and R. R. Xu, *Adv. Mater.*, 1999, **11**, 1091.
26 S. X. Liu, H. Y. He, Z. H. Luan and J. Klinowski, *J. Chem. Soc., Faraday Trans.*, 1996, **92**, 2011.
27 J. Rocha, P. Brandao, M. W. Anderson, T. Ohsuna and O. Terasaki, *Chem. Commun.*, 1998, 667.
28 C. Fild, D. F. Shantz, R. F. Lobo and H. Koller, *Phys. Chem. Chem. Phys.*, 2000, **2**, 3091.
29 Y. Z. Khimyak and J. Klinowski, *Phys. Chem. Chem. Phys.*, 2001, **3**, 1544.
30 D. Zhao, Z. Luan and L. Kevan, *J. Phys. Chem. B*, 1997, **101**, 6943.
31 Z. Luan, D. Zhao, H. He, J. Klinowski and L. Kevan, *Stud. Surf. Sci. Catal.*, 1998, **117**, 103.
32 Z. Luan, D. Zhao, H. He, J. Klinowski and L. Kevan, *J. Phys. Chem. B*, 1998, **102**, 1250.
33 B. Chakraborty, A. C. Pulikottil, S. Das and B. Viswanathan, *Chem. Commun.*, 1997, 911.
34 G. Horvath and K. Kawazoe, *J. Chem. Eng. Jpn.*, 1983, **16**, 470.
35 Y. Z. Khimyak, *Ph.D. Thesis*, University of Cambridge, Cambridge 2000, p. 276.
36 Y. Z. Khimyak and J. Klinowski, *Phys. Chem. Chem. Phys.*, 2001, **3**, 2544.
37 A. Sayari, I. Moudrakovski, C. Danumah, C. I. Ratcliffe, J. A. Ripmeester and K. F. Preston, *J. Phys. Chem.*, 1995, **99**, 16373.
38 S. Kroeker and J. F. Stebbins, *Inorg. Chem.*, 2001, **40**, 6239.
39 S. M. DePaul, M. Ernst, J. S. Shore, J. F. Stebbins and A. Pines, *J. Phys. Chem. B*, 1997, **101**, 3240.
40 S. E. Ashbrook, J. McManus, K. J. D. MacKenzie and S. Wimperis, *J. Phys. Chem. B*, 2000, **104**, 6408.
41 C. Fild, H. Eckert and H. Koller, *Angew. Chem., Int. Ed.*, 1998, **37**, 2505.